Received: 4 September 2020 | Revised: 29 December 2021 | Accepted: 6 January 2022

DOI: 10.1002/hyp.14475

RESEARCH ARTICLE

WILEY

Isolating forest process effects on modelled snowpack density and snow water equivalent

Hannah M. Bonner[1] | Mark S. Raleigh[2] | Eric E. Small[1]

[1]Department of Geological Sciences, University of Colorado, Boulder, Colorado, USA

[2]College of Earth, Ocean, and Atmospheric Sciences, Oregon State University, Corvallis, Oregon, USA

Correspondence
Hannah M. Bonner, Department of Geological Sciences, University of Colorado, Boulder, CO, USA.
Email: hannah.bonner@colorado.edu

Funding information
Division of Earth Sciences, Grant/Award Number: 1761441

Abstract

Understanding how the presence of a forest canopy influences the underlying snowpack is critical to making accurate model predictions of bulk snow density and snow water equivalent (SWE). To investigate the relative importance of forest processes on snow density and SWE, we applied the SUMMA model at three sites representing diverse snow climates in Colorado (USA), Oregon (USA), and Alberta (Canada) for 5 years. First, control simulations were run for open and forest sites. Comparisons to observations showed the uncalibrated model with NLDAS-2 forcing performed reasonably. Then, experiments were completed to isolate how forest processes affected modelled snowpack density and SWE, including: (1) mass reduction due to interception loss, (2) changes in the phase and amount of water delivered from the canopy to the underlying snow, (3) varying new snow density from reduced wind speed, and (4) modification of incoming longwave and shortwave radiation. Delivery effects (2) increased forest snowpack density relative to open areas, often more than 30%. Mass effects (1) and wind effects (3) decreased forest snowpack density, but generally by less than 6%. The radiation experiment (4) yielded negligible to positive effects (i.e., 0%–10%) on snowpack density. Delivery effects on density were greatest at the warmest times in the season and at the warmest site (Oregon): higher temperatures increased interception and melted intercepted snow, which then dripped to the underlying snowpack. In contrast, mass effects and radiation effects were shown to have the greatest impact on forest-to-open SWE differences, yielding differences greater than 30%. The study highlights the importance of delivery effects in models and the need for new types of observations to characterize how canopies influence the flux of water to the snow surface.

KEYWORDS
bulk snow density, canopy interception, forest snow density, mountain forests, snow climates, snow modelling, SUMMA, SWE

1 | INTRODUCTION

Accurately predicting snow water equivalent (SWE) is central for managing water resources. Because more than half of the snow in the Western USA accumulates in forested areas (Oswalt & Smith, 2014), characterizing forest effects on snowpack characteristics is critical. The presence of a forest canopy changes how much snow reaches the ground, the phase and density of the snow that reaches the ground, wind packing of new snow, and the surface energy balance available to warm and melt the snowpack. We examine how these factors influence the bulk density of snowpack and result in SWE differences between forest and open areas.

TABLE 1 Characteristics of the three sites used in the modelling experiments

Location	Years modelled	Coordinates	Mean Nov.-March temperature (C)[x]	Mean Nov.-March precipitation (mm)[x]	Mean peak SWE (mm)[x]	Forest LAI*	Height of canopy (m)*	Intercepted precipitation lost to evaporation or sublimation (%)*
Snodgrass Mountain, Colorado, USA	2014–2018	38.9274, −106.9777	−3.1	325	565	4	9	12
McKenzie River basin, Oregon, USA	2011–2015	44.4130, −121.8524	1.5	1256	473	1	14	3
Marmot Creek basin, Alberta, Canada	2012–2016	50.9569, −115.1762	−5.7	203	218	4	8	34

Note: Columns with * indicate SUMMA values from control simulations. Columns with [x] indicate values downloaded from a SNOTEL station located near the site.

Snow density is a critical component in informing SWE estimates from retrievals such as lidar-based snow depth (Deems et al., 2013; Harpold et al., 2014; Hopkinson et al., 2001; Painter et al., 2016) and ground-penetrating radar (Lundberg et al., 2016; St. Clair & Holbrook, 2017; Webb et al., 2020). However, while the effects of forests on SWE have been well studied (see reviews: Lundquist et al., 2013; Varhola et al., 2010), less attention has been given to understanding how forest canopies affect snowpack density. Past field studies have yielded inconsistent results in terms of how snow density varies between forest and open areas. Observed density differences have been attributed to either mass, delivery, wind, or radiation effects (Lundberg & Koivusalo, 2003; Rasmus, 2013). 'Mass effects' result from canopy interception loss, reduced snow mass on the ground, and subsequently lower compaction rates and lower density (Marchand & Killingtveit, 2004; Schöber et al., 2016; Timoney et al., 1992; Winstral & Marks, 2014). 'Delivery effects' on density, are caused when snowfall is intercepted by the canopy and then later added to the underlying snowpack as meltwater drip or unloaded snow that may have a higher density than fresh snowfall (Bründl et al., 1999; Lundberg et al., 1997; Storck et al., 2002). 'Wind effects' occur when wind speed is reduced by the forest structure resulting in lower snow density relative to exposed open areas where wind packing can densify falling snow and the snow surface (Pahaut, 1976; Pomeroy & Gray, 1995). 'Radiation effects', caused by altered shortwave and longwave fluxes under a forest canopy, may increase or decrease snow density through changes in snow temperature, snowpack temperature gradients, and melt-refreeze cycles (Essery et al., 2008; Lawler & Link, 2011; Sicart et al., 2004). Understanding the contributions of mass, delivery, wind, and radiation effects in determining the density of snow under a forest canopy is important for process representation in modelling and improving retrievals of SWE from remote sensing.

In this paper, we examine how forests influence mountain snowpack density and SWE (relative to open areas), using the SUMMA (Structure for Unifying Multiple Modelling Alternatives) model (Clark et al., 2015a, 2015b) to mechanistically investigate mass, delivery, wind, and radiation effects. To compare the effects in different climates and forest types, we conduct point-scale modelling experiments at three locations: Snodgrass Mountain, Colorado (continental climate); the Marmot Creek basin, Alberta (intermountain climate); and the McKenzie River basin, Oregon (maritime climate; Table 1, Section S1). The modelling experiments are designed to address the question: How do individual forest canopy processes affect snow density and SWE on the ground? These experiments reveal potential gaps in our understanding of the relative importance of forest processes, which cannot be readily isolated with typical field measurements. This is primarily a modelling study, but we also compared simulations to field data at the three sites to assess model performance.

2 | MODEL REPRESENTATION

The SUMMA model (version 2.0.0) was chosen to explore the effect of forest canopies on snow densification and SWE (Clark et al., 2015a, 2015b). SUMMA is modular and can be reconfigured into a wide range of process representation alternatives. These features have been used to isolate individual processes and diagnose model error (Wayand

et al., 2017). SUMMA is similar to other multi-physics models, including FSM (Essery, 2015) and ESCROC (Lafaysse et al., 2017), and simultaneously represents multiple processes driving the hydrologic cycle. SUMMA's representation of snowpack density, and forest mass, delivery, wind, and radiation effects, will be briefly discussed here and further detailed in supplement sections S2–S6.

2.1 | Snowpack density

The density of snow on the ground changes through the season due to a combination of processes: overburden compaction and settling (Chen & Baker, 2010; Lundberg et al., 2006; Winstral & Marks, 2014), new precipitation (Judson & Doesken, 2000; McCreight & Small, 2014), wind compaction (Sommer, 2018; Sommer et al., 2018), snowmelt and melt-freeze cycles (Colbeck, 1982), and grain growth from metamorphism (Anderson, 1976; Gray & Morland, 1995; Jordan, 1991; Raymond & Tusima, 1979). These processes are directly or indirectly affected by the presence of a forest canopy.

SUMMA calculates snowpack density on a per layer basis for each hourly timestep, using a maximum of five snowpack layers, as in the Community Land Model scheme (Lawrence et al., 2011; Section S2). The density of the *i*th snow layer is calculated based on the layer volumetric fraction of ice (f_{ice}) and the layer volumetric fraction of liquid (f_{liq}):

$$\rho_{snow,i} = f_{ice} * \rho_{ice} + f_{liq} * \rho_{liq}, \quad (1)$$

SUMMA calculates changes in density (and thus layer thickness) from grain growth via metamorphism and overburden compaction. Changes in layer density from compaction are ~10–100 times greater than those from grain growth. Densification rates are fastest when the snow is warm and ice fraction (or layer density) is low (Figure 1a, b). SUMMA also calculates changes in layer thickness, and any associated increases in density, from melt, refreezing, and sublimation. These increases are similar in magnitude to changes from overburden compaction. The bulk snowpack density is calculated using all layers, weighted by their relative thickness.

2.2 | Mass effects

Forest canopies intercept snowfall, some of which evaporates or sublimates. These canopy 'mass effects' reduce the mass of snow (i.e., SWE) beneath forests relative to adjacent open areas (Timoney et al., 1992; Varhola et al., 2010). As indicated by observations and represented in SUMMA, reduced snow mass under the forest canopy reduces the rate of overburden compaction (Figure 1a; Bader, 1960; Bormann et al., 2013; Sturm & Holmgren, 1998). Consequently, model representation of mass effects relies on accurate predictions of canopy interception with parameterization suited to site climate. We used the representation from Hedstrom and Pomeroy (1998) for our continental and intermountain sites and Andreadis et al. (2009) for our maritime site (Section S3). SUMMA simulations of mass loss from

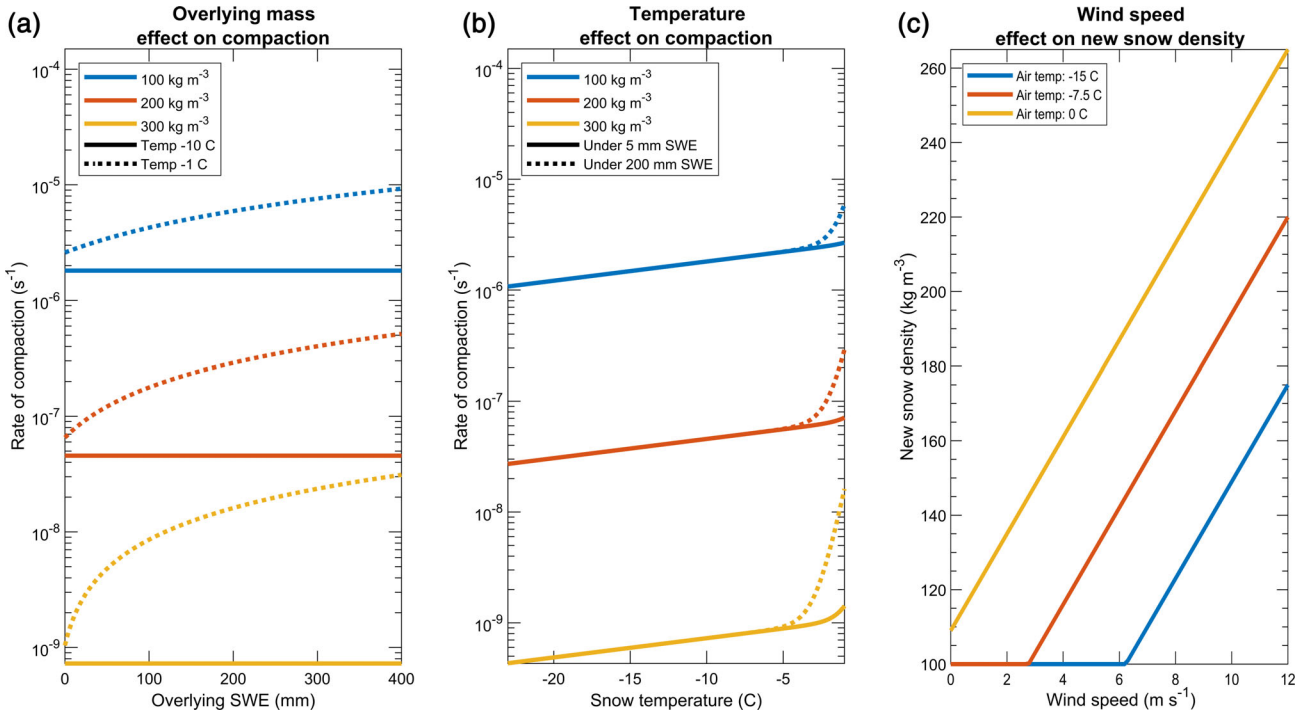

FIGURE 1 SUMMA model mechanics: The effect of overlying mass on the overburden compaction rate parameter (a); the effect of snow temperature on the overburden compaction rate parameter (b); the effect of wind speed on new snow density as represented by the Pahaut (1976) parameterization (c)

forest canopy interception and sublimation/evaporation varied between site and specific storm event (Table 1).

2.3 | Delivery effects

Canopies affect both the phase (solid versus liquid) and the density of snow that reaches the forest floor (i.e., 'delivery effects'). If not lost to evaporation or sublimation, intercepted snow resides in the canopy on the timescale of hours to days before being delivered to the underlying snowpack, either as unloaded snow or draining melt water (Storck et al., 2002). Delivery effects may increase forest snow density in two ways. First, while in the canopy, intercepted snow may be exposed to higher shortwave energy than snow under the canopy, increasing the potential for melt or melt-refreeze (Sicart et al., 2004). Second, the process of unloading may change the surface structure of the underlying snowpack (e.g., compressed layers or voids; Bründl et al., 1999; Teich et al., 2019). To represent the first of these processes, SUMMA calculates the energy flux available to generate liquid drainage and the ratio of water unloaded as snow vs. melt drip. Snow that melts in the canopy and then drains into the underlying snowpack has the density of liquid water. In partial representation of the second process, SUMMA also increases the density of unloaded snow. Irrespective of residence time in the canopy, unloaded snow is assigned a density of 200 kg m^{-3} as it joins the underlying snowpack. This is nearly twice the average new snow density received in the absence of a canopy, and thus important to delivery effects (Section S6).

2.4 | Wind effects

Wind speed influences the density of new/fresh snow and the subsequent compaction of the snowpack from drifting (Figure 1c; Kozlov, 2001; Sturm et al., 2001). Wind sheltering in forests (i.e., 'wind effects') reduces wind speed and diminishes wind-driven snow densification (Liston & Sturm, 1998; Male & Gray, 1981). SUMMA represents wind sheltering by calculating a wind speed profile and reducing wind speed through the canopy using a logarithmic decay function. Wind speed at the bottom of simulated forest canopies is, on average, only 3% of the forcing wind speed. This sheltering results in wind effects on snow density, represented by the Pahaut (1976) equation: calculated new snow density is decreased in forested areas relative to open areas, due to comparatively lower wind speed (Figure 1c; Section S4). SUMMA, like most snow models, does not represent densification from snowpack drifting.

2.5 | Radiation effects

Forest canopies block incoming shortwave radiation and emit additional longwave radiation downward towards the snow surface (Harding & Pomeroy, 1996; Hardy et al., 2004). This modulates snowpack temperature, reduces the diurnal range of near-surface temperature, affects the rate of densification via thermal controls on snow viscosity, and limits the continuity of melt-freeze crusts found in forests (Anderson, 1976; Teich et al., 2019; Figure 1a, b). Radiation regime also controls the timing of snowpack melt, which facilitates a period of rapid densification. Here, we refer to 'radiation effects' as the sum of these changes on snowpack density, relative to what exists in the absence of a forest canopy. In response to the presence of forest cover, SUMMA alters shortwave and longwave fluxes reaching the underlying snowpack. Incoming shortwave is reduced based on canopy density using the two-stream radiative transfer model of Dickinson (1983) and Sellers (1985) as implemented in the Community Land Model scheme (Lawrence et al., 2011). In contrast, incoming longwave is generally increased as the canopy radiates higher thermal energy (relative to the atmosphere). Longwave fluxes from forest vegetation are calculated using Mahat and Tarboton's (2012) expression, which calculates emissivity using the transmissivity of diffuse shortwave radiation. These radiation effects are part of a broader energy regime, but while sensible and latent heat fluxes may also vary in the forest setting, they are expected to be of secondary importance (Marks & Winstral, 2001; Stoy et al., 2018).

3 | STUDY DATA AND EXPERIMENTAL DESIGN

Three sites with distinct climates were selected for experiments (Table 1). While diverse global snow climates exist (Sturm et al., 1995), we focused on three mountainous sites with distinct snowpack regimes (Trujillo & Molotch, 2014), snow density characteristics (Mizukami & Perica, 2008), and forest types. Sites were also selected for historic availability of snow density and SWE field observations. Snodgrass Mountain (CO, USA) is within the continental climate region with dry, lower density snow. The McKenzie River basin (OR, USA) is within the maritime climate region with wet, higher density snow. The Marmot Creek basin (Alberta, Canada) is in the intermountain region with snow characteristics distinct from the other two sites (Section S1). These sites will hereafter be referred to as 'Colorado', 'Oregon', and 'Alberta,' respectively.

Forcing data (precipitation, incoming shortwave and longwave radiation, air temperature, wind speed, atmospheric pressure, and specific humidity) were sourced from hourly 1/8-degree data from NLDAS-2 (North American Land Data Assimilation System phase 2; Xia et al., 2012) and downscaled to the study site locations using the MeteoIO preprocessing library (Bavay & Egger, 2014; Essery, 2015). Local meteorological observations from the sites were of varying completeness, and were only used to compare against the downscaled forcing data (Section S7). Downscaled NLDAS-2 data were sufficient for this study, which focuses on understanding processes within a modelling framework, not reproducing observations at particular sites.

Control simulations were the basis of comparison for the mass, delivery, wind, and radiation effects experiments. At each site,

TABLE 2 Summary of model densification process experiments and parameter sensitivities

Experiment name	Starting conditions	Change to model
Control open	Control open	None
Control forest	Control forest	None
Mass effects	Control open	Incoming precipitation scaled down to mimic sublimation/evaporation loss of snow intercepted by canopy
Delivery effects	Control open	Incoming snowfall density adjusted to reflect densification from canopy unloading and drip
Wind effects	Control open	Sub-canopy wind speed used in calculating new snow density reduced to 3% of forcing to imitate forest wind speed profile
Radiation effects	Control open	Altered forcing datasets used for shortwave and longwave fluxes to imitate canopy effects on radiation

SUMMA was configured to run for one point that represented open conditions (control open) and another for forest conditions (control forest; Table 2). The same downscaled forcing data were used as input for both, but SUMMA altered forcing data (e.g., surface radiation, wind speed) to account for canopy effects (see below). We used a representative canopy height and leaf area index (LAI) value at each site (Table 1, Section S1). All sites were modelled as flat ground. Model simulations, occurring at hourly timesteps, began on November 15 and ended on July 31. Each site was modelled for five consecutive water years (each year independently): 2014–2018 for Colorado, 2012–2016 for Alberta, and 2011–2015 for Oregon. In addition, Colorado was modelled for water year 2019, but these results were used solely for comparison to our field observations. Alberta and Oregon were compared to field observations during 2012–2016 and 2011–2015, respectively.

3.1 | Mass effects experiment

We started with the control open setup (i.e., no forest canopy), and then reduced the precipitation input by a prescribed percentage to reflect average annual interception losses across 5 years (Tables 1, 2). The reduction in precipitation was calculated by comparing the control open and control forest experiments (Section 4.1). Comparing the mass effects experiment to the control open simulations allowed us to isolate how canopy interception losses impact snow densification via reduced snow mass on the ground. The control open and mass effects experiments were otherwise identical in terms of delivery, wind, and radiation effects.

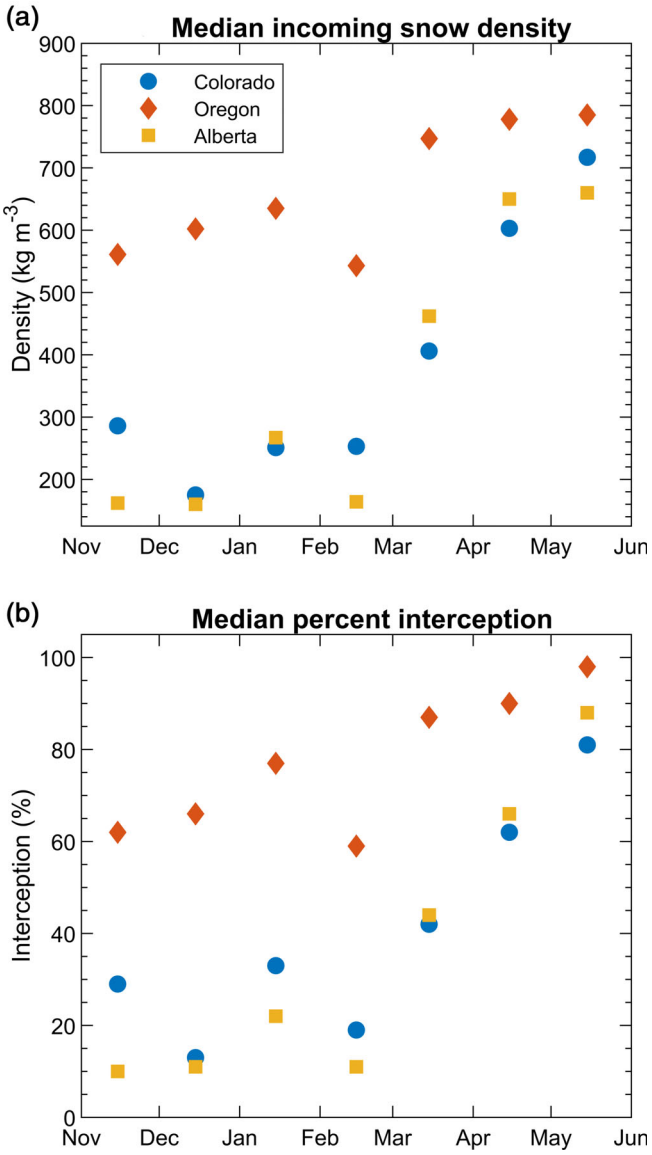

FIGURE 2 Monthly values of median density of total delivered snow (a) and canopy interception percent (b) at control forest for the three study sites. Here, 'total delivered snow' includes direct throughfall, canopy unloading of snow mass, and liquid drainage of melted intercepted snowfall (equation 2). Year-specific values were used in modelling experiments, which differ from the median values shown here based on 5-years of data at each site

3.2 | Delivery effects experiment

SUMMA was run using control open conditions but with modified new snowfall density values (Table 2; Figure 2a). The modified new snowfall density values were calculated monthly as follows:

$$\rho_{del} = f_{tf}\rho_{tf} + f_{int}\rho_{int} + f_{liq}\rho_{liq}, \quad (2)$$

where f is the fraction of water in the control forest experiment reaching the ground from throughfall (tf), unloading of intercepted

snow (*int*), and canopy melt (*liq*), and ρ is the density of each component. Thus, the delivery effects experiment had the mass, wind, and radiation of control open, but the input snow density was equivalent to typical values from forest simulations.

3.3 | Wind effects experiment

SUMMA was run using control open conditions, but with an altered wind speed used for the Pahaut new snow density equation. Forcing wind

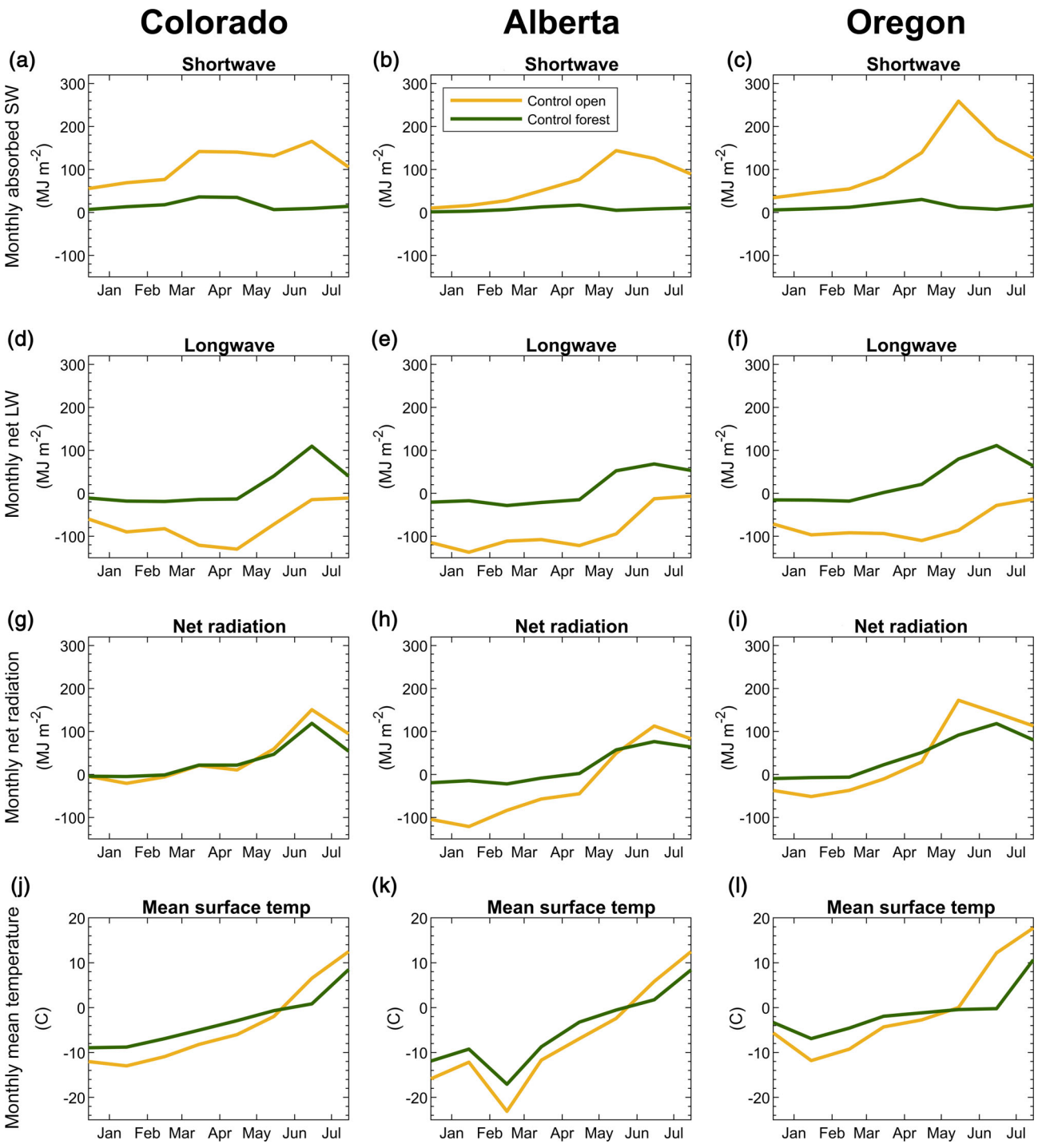

FIGURE 3 Comparison of net shortwave (a–c), net longwave (d–f), net radiation (g–i), and temperature (j–l) at the snow surface in control open and control forest conditions at the three study sites. Data from a typical water year is shown (Colorado, WY 2015; Alberta, WY 2014; Oregon, WY 2013). For shortwave, longwave, and net radiation, monthly sums were calculated. For mean surface temperature, the monthly mean was calculated

speed was multiplied by 0.03 to replicate the reduction of wind speed beneath the canopy in the control forest simulation. Comparing the wind effects experiment to control open simulations allowed us to isolate the effects of reduced forest wind speed on new snow density.

3.4 | Radiation effects experiment

We used the control open setup, but ran the model using a canopy-altered radiation forcing data set, constructed by modifying the downscaled NLDAS radiation values. We created this data set using SUMMA outputs of net shortwave and longwave fluxes reaching the ground under control forest conditions (Figure 3; Section 2.5). The resulting experiment had incoming radiation similar to control forest, but otherwise the same mass, delivery, and wind characteristics of control open. This design allowed us to isolate the effects of canopy-altered radiation on snow density, while maintaining the same approach (e.g., a modified control open setup) as the other experiments.

3.5 | Analysis and sensitivity

We summarized differences between experiments and control simulations using two metrics for each water year: median density difference (DM) and median SWE difference (SM).

$$DM\,or\,SM = \frac{M_{exp} - M_{control}}{M_{control}} * 100, \quad (3)$$

DM and SM were obtained by subtracting the yearly median of control open ($M_{control}$) from the yearly median of each experiment (M_{exp}), excluding data from times when snowpack depth in either simulation was less than 15 cm. The resulting value was then divided by the yearly median of control open ($M_{control}$) and multiplied by 100 to normalize results. DM and SM values reflect percent difference between 1 year of an experiment and the corresponding year of control open. For example, if 1 year of an experiment simulation had a DM of 20, that indicated that the yearly median density was 20% higher in the experiment than in control open. DM and SM were also calculated for control forest to gauge the combined effects of all four-forest processes.

Sensitivity experiments were run to determine how results were impacted by parameter selection or magnitude of perturbation. Each experiment was analysed for parameter values of greatest sensitivity. Field measurements, values from the literature, and SUMMA's provided maximum/minimum values were used to set reasonable ranges for these parameters (Table 3). The experiments were then repeated twice for each site and year using the range's endmember values. Although the ranges used were subjective, larger variations lead to unrealistic values for model states such as density. Results from sensitivity experiments were used to calculate a set of possible DMs and SMs.

4 | RESULTS

4.1 | Control open and control forest

We first compared the control open and control forest simulations to demonstrate the integrated effects of all forest canopy processes on snowpack evolution. Based on winter temperature and precipitation, we selected representative years from Colorado, Alberta, and Oregon (2015, 2014, and 2013, respectively; Figure 4).

Snow density differences varied in sign throughout each of the example years shown (Figure 4d–f). In general, the model had higher density in control forest than control open at Colorado and Oregon and lower density in control forest than control open at Alberta. Density differences were largest at Oregon, with bulk density up to 40 kg m^{-3} greater in the forest than the open until April. At Colorado and Alberta, forest-open differences were typically less than 20–30 kg m^{-3}. At all three sites, SWE was consistently higher in control open than in control forest during the accumulation season, with the magnitude of the difference increasing storm-by-storm. This indicated interception losses in the forest reduced snow mass on the ground, relative to the open. Through the ablation season, SWE declined more rapidly in control open for all sites, as a consequence of the forest canopy reducing net radiation for snowmelt (Figure 4a–c). Snow depth differences between forest and open exhibited similar, but not identical, patterns as SWE (Figure 4g–i).

4.1.1 | Interception loss

Using control forest, we calculated interception loss by summing canopy sublimation and evaporation. As a percent of precipitation, the

TABLE 3 Sensitivities considered for modelling experiments

Experiment name	Parameter/perturbation varied	Range considered
Mass effects	Temperature overburden scaling value	0.064–0.096 (±20%)
	Density overburden scaling value	0.0184–0.0276 (±20%)
Delivery effects	Percent ± of material unloaded as liquid drip	80%–120%
Wind effects	Minimum new snow density value	50–100 kg m^{-3}
Radiation effects	Percent ± of incoming longwave radiation	95%–105%
	Percent ± of incoming shortwave radiation	95%–105%

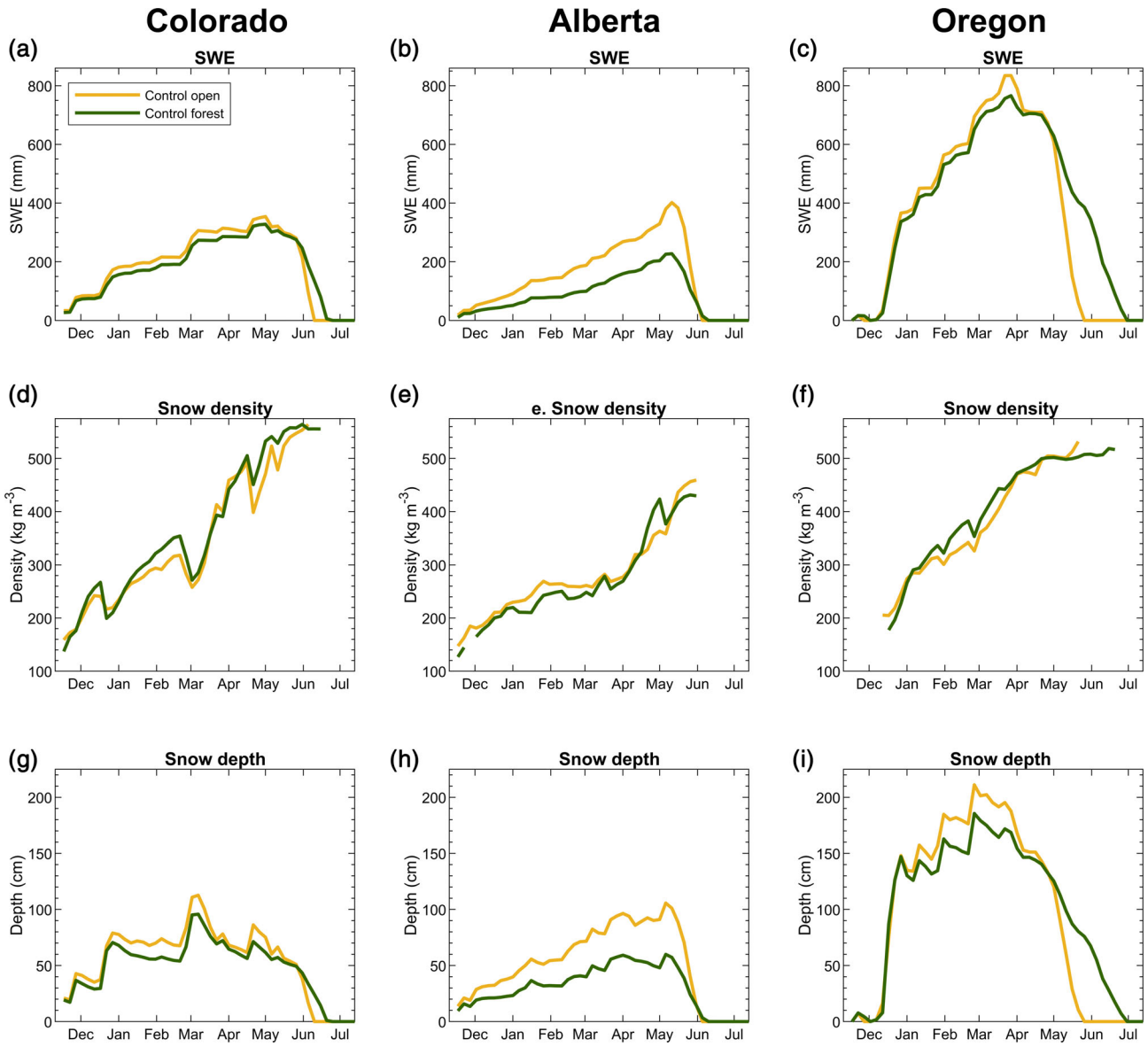

FIGURE 4 SUMMA generated time series of SWE (a–c), bulk density (d–f), and depth (g–i) for control forest and control open model runs at the three study sites during a typical water year (Colorado, WY 2015; Alberta, WY 2014; Oregon, WY 2013). Results are smoothed by calculating median values over a 5-day period to clarify forest versus open differences. Density values are only shown when snowpack is at least 15 cm in depth

sum of canopy sublimation and evaporation was greatest at Alberta (34% of precipitation), followed by Colorado (12% of precipitation), and lowest at Oregon (3% of precipitation; Table 1). These interception loss results guided the mass effects experiments.

4.1.2 | Transfer of snow and liquid water under the canopy

We determined the effective density of water delivered to the snow surface under the canopy based on Equation 2, for use in the delivery effects experiment. Precipitation delivered as rainfall was not considered. At Colorado and Alberta, the density of this snow-liquid mixture was ~150–250 kg m^{-3} during the accumulation season (Figure 2a). This indicated that most of the canopy-to-snowpack transfer during this interval was unloaded snow, which appeared as higher density layers added to the snow surface in the forest following storms (Figure 5b). These higher density layers were absent in the control open simulation (Figure 5a). Through the ablation season, effective density increased at Colorado and Alberta (Figure 2a) as more intercepted snow melted, and warmer temperatures facilitated increased interception capacity (Figure 2b). This canopy melt caused high-density surface snow in the Colorado forest (yellow region, Figure 5b), weeks before the snowpack was isothermal and snowpack melt began. In contrast, at Oregon, the effective density of water delivered to the forest floor was over 500 kg m^{-3} throughout the water year.

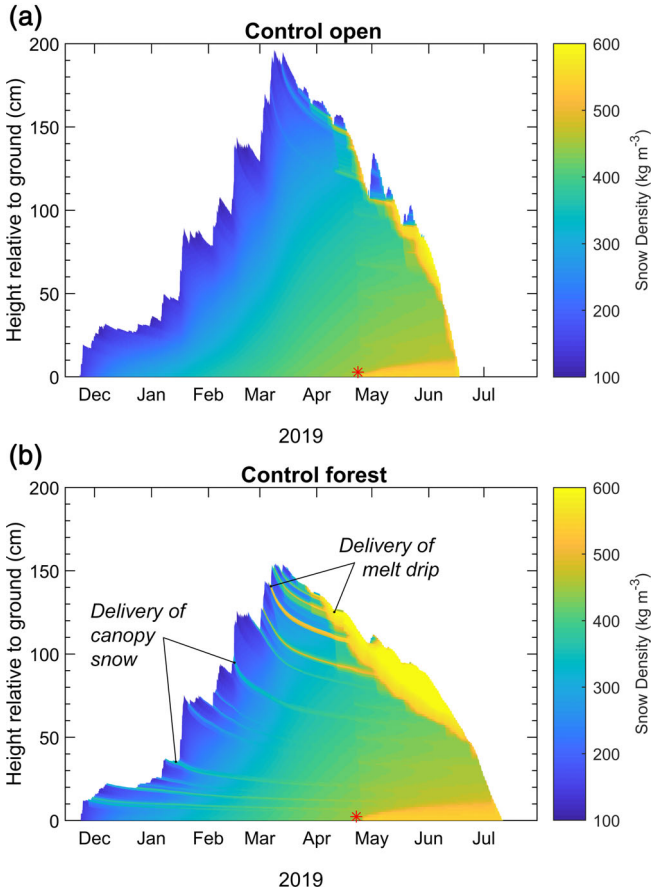

FIGURE 5 Modelled vertical profile of snow density through time for control open (a) and control forest (b) at the Colorado site during water year 2019. The red asterisk represents when the snowpack has gone isothermal

Oregon is a warmer site, so more than half of intercepted snow melted in the canopy and was delivered as liquid water to the snowpack. The interception efficiency was also 20%–40% higher at Oregon (Figure 2b) than at the two colder sites, due to differences in climate and the interception parameterization used.

4.1.3 | Radiation and temperature

Forest-to-open differences in radiation had similar patterns at the three sites. During the early accumulation season, monthly net shortwave was up to 45 MJ m^{-2} higher in the open than the forest (Figure 3a–c). Net longwave was higher in the forest by a similar amount at Colorado and 60–100 MJ m^{-2} at Alberta and Oregon (Figure 3d–f). In the ablation season, the increase in net shortwave yielded higher net radiation in the open (Figure 3g–i), leading to the more rapid melt simulated in control open (Figure 4g–i). Until mid-May, surface temperatures of the snowpack were on average several degrees warmer in control forest than in control open (Figure 3j–l). The greatest temperature differences occurred at night, when the elevated longwave radiation from the forest canopy kept the snowpack warmer (not shown).

4.2 | Comparison to field observations

To evaluate the representativeness of the control simulations and to contextualize the results, we compared simulations to field observations from the three sites. Data used for Colorado was collected during four field visits during 2019. At each visit, standard snow pit measurements were completed at seven pits each in forested and open areas (Section S1). Five years of historic data sourced from work by Fang et al. (2019) and Roth and Nolin (2017) were used respectively for comparison to Alberta and Oregon results. These data contained measurements taken along established snow transects in the forest and open.

Observational data were used to calculate root mean squared errors (RMSE) for SUMMA predictions of SWE at Colorado in 2019, Alberta in 2011–2015, and Oregon in 2011–2016. RMSE were normalized by dividing the RMSE by the standard deviation of SWE observations, for comparison to snow model evaluations in SnowMIP2 (Rutter et al., 2009). While SUMMA's performance may have been improved by optimizing model parameters and using local meteorological inputs (though minimally, see Section S7), we found that in both its control open and control forest configuration, SUMMA performed well at all three sites. When compared to both calibrated and uncalibrated models in SnowMIP2, SUMMA had above average performance at Colorado and Oregon and average performance at Alberta (Table S4, S5; Section S8). The performance of SUMMA in representing snow density was also comparable to or better than other models documented in recent studies (Lv & Pomeroy, 2020; Terzago et al., 2020).

We focused on the differences in density, depth, and SWE between open and forest sites, to gauge if SUMMA's representation of net forest effects was consistent with observations. Figure 6 compares modelled and observed differences at Colorado, Alberta, and Oregon during a representative year (2019, 2014, and 2013, respectively). The simulated forest-to-open differences in bulk density were generally within 10–40 kg m^{-3} of observed differences at Colorado and Alberta. More variation existed at Oregon, especially during April when SUMMA predicted greater density in the forest than open, but observations showed greater density in the open. A similar offset occurred at the Colorado site's April observation date and the Alberta site's May observation dates. The discrepancies between modelled and measured snow density may reflect imperfections in model representation or inadequacies of standard field sampling protocols (see Spittlehouse and Winkler (1996); Watson et al. (2006); Section S9). SUMMA predictions of snow depth at Colorado matched observations at the beginning and end of the snow season, but mid-water year predicted less snow in control forest than was observed. In contrast, modelled snow depth differences at Alberta fit well with the observation pattern throughout the water year, but were slightly offset in timing: snow depth peaked later than observed. Oregon model differences also fit the observed pattern with a temporal offset as they predicted snow depth peaking later than observed and predicted less snow in control forest than observed mid-water year. SUMMA performed well at simulating forest-to-open SWE differences at Colorado and Alberta with disagreement between modelled results and observations generally less than 50 mm. SUMMA also captured SWE

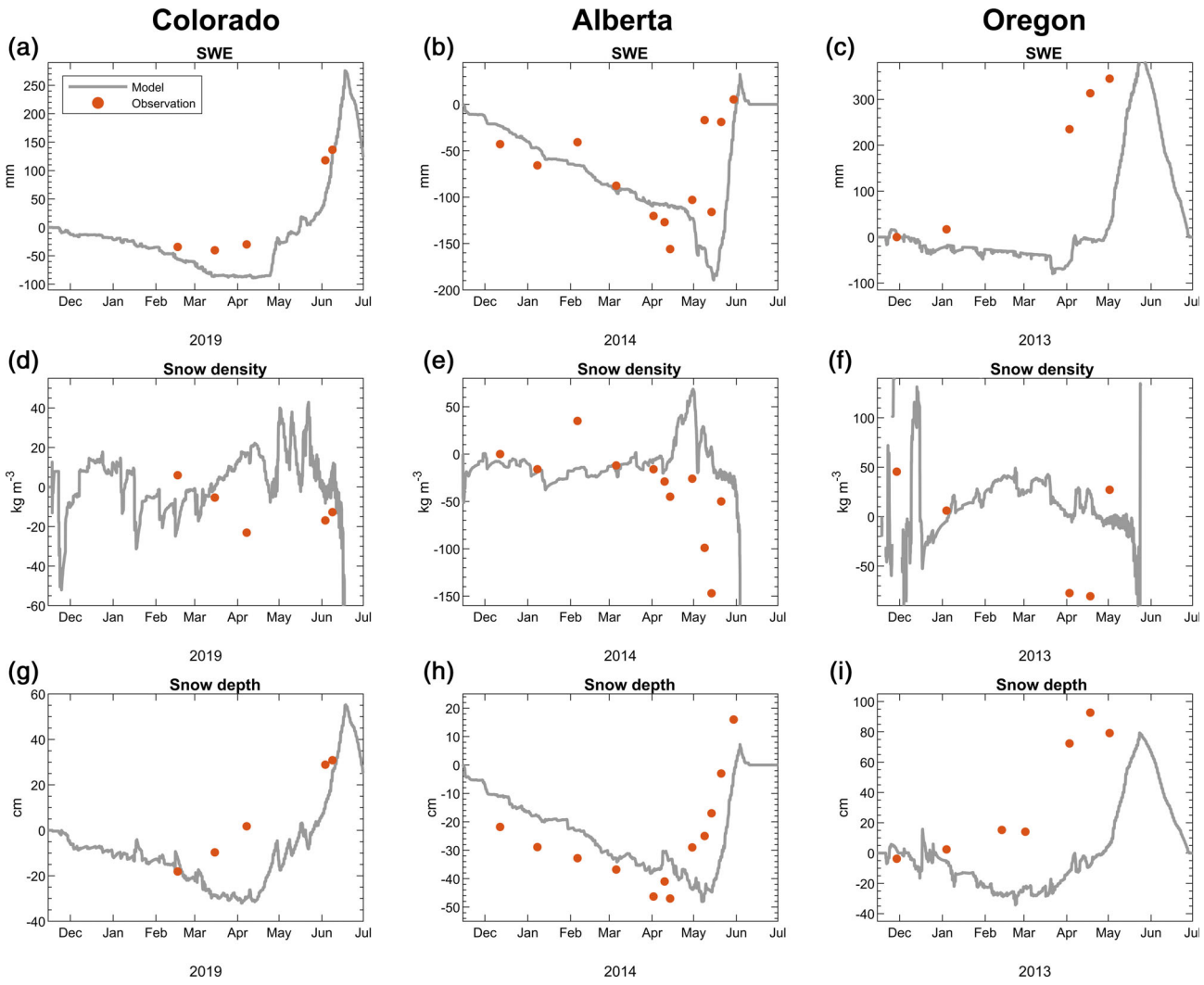

FIGURE 6 The difference between control forest and control open model runs at the three study sites during a representative water year (Colorado, WY 2019; Alberta, WY 2014; Oregon, WY 2013). Differences in SUMMA outputs of SWE (a–c), density (d–f), and depth (g–i) are shown. Corresponding field observation differences are indicated with circular markers

differences well during the accumulation season at Oregon, but as a result of delayed snow melt in control open, was offset in peak difference timing.

4.3 | Mass effects experiment

We next calculated median density difference (DM) and median SWE difference (SM) metrics for experiments and control forest at each site and year considered. These results show the overall impact of each experiment as well as year-to-year variations and parameter sensitivity (Figures 7, 8). A time series of density and SWE differences between control open and each experiment was also created (Figures 9, 10).

4.3.1 | Density

The imposed decrease in precipitation in the mass effects experiment, resulted in bulk density values lower than control open throughout most the year at all sites (Figures 7, 9). Yearly median density difference metrics (DM) were consistently negative and showed a 1%–12% difference between experiment and control open density (Figure 7). The one exception was that density was slightly higher than control open during the ablation season at Colorado and Alberta, as the snowpack's reduced SWE resulted in an earlier onset of melt and melt densification (Figure 9). When sensitivity to compaction parameters was considered, DMs were slightly larger (see length of whiskers in Figure 7).

4.3.2 | Snow water equivalent

As expected, the mass effects experiment yielded 4%–36% lower SWE than control open due to the imposed loss of incoming snow. The loss of SWE was observed for all sites and years, as shown by yearly median SWE difference metrics (SM; Figure 8), and generally increased through the season (Figure 10). Across sites and years, SMs were not sensitive to choice of compaction parameters.

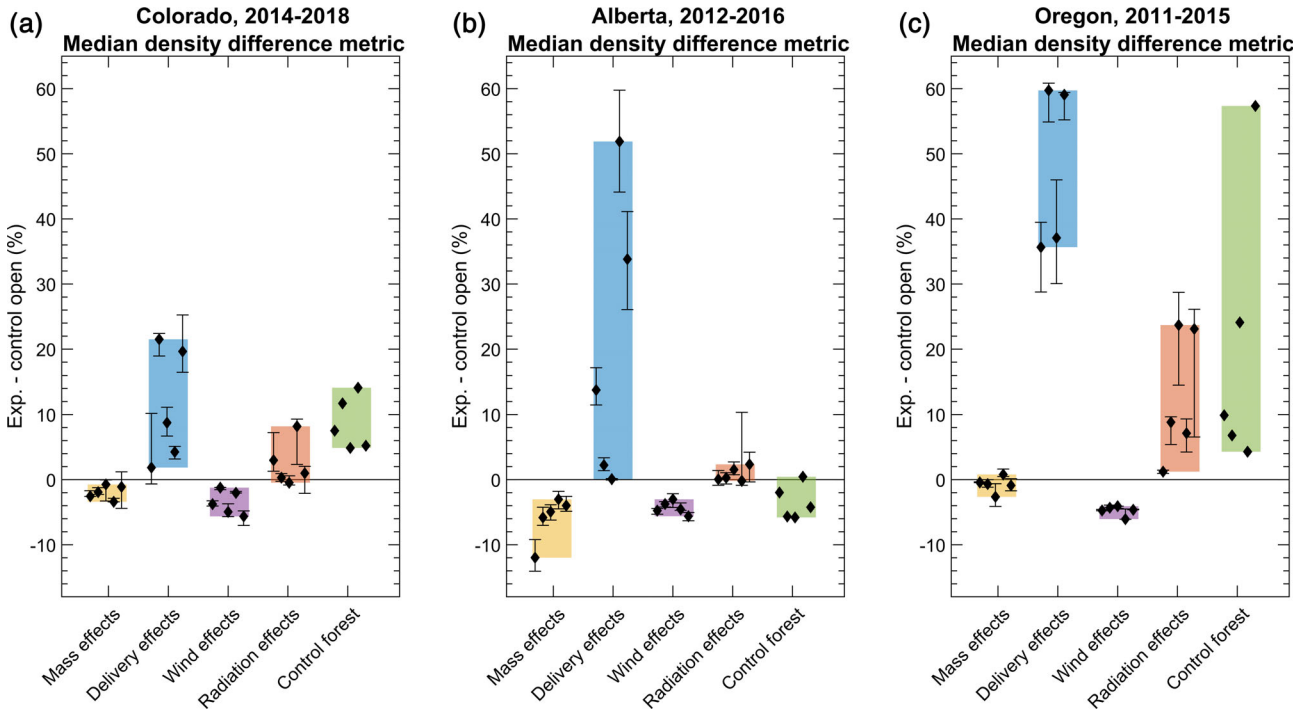

FIGURE 7 Median density difference metrics (DM) at the three sites. Vertical axis is percent difference between experiment and control open (Equation 3). Each diamond represents a different year in the 5-year period and is bracketed with whiskers showing metric sensitivity to tested parameter variation (Table 3). Results are clustered by experiment

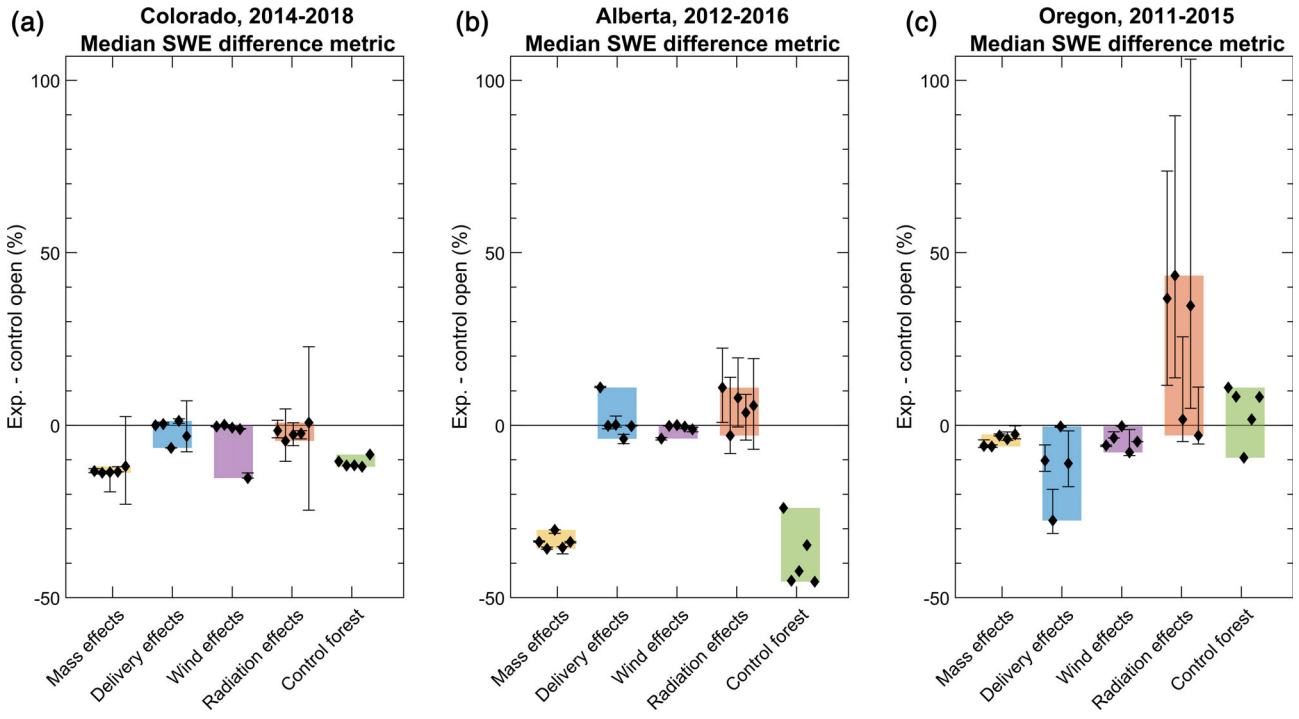

FIGURE 8 Median SWE difference metrics (SM) at the three sites. Vertical axis is percent difference between experiment and control open (equation 3). Each diamond represents a different year in the 5-year period and is bracketed with whiskers showing metric sensitivity to tested parameter variation (Table 3). Results are clustered by experiment

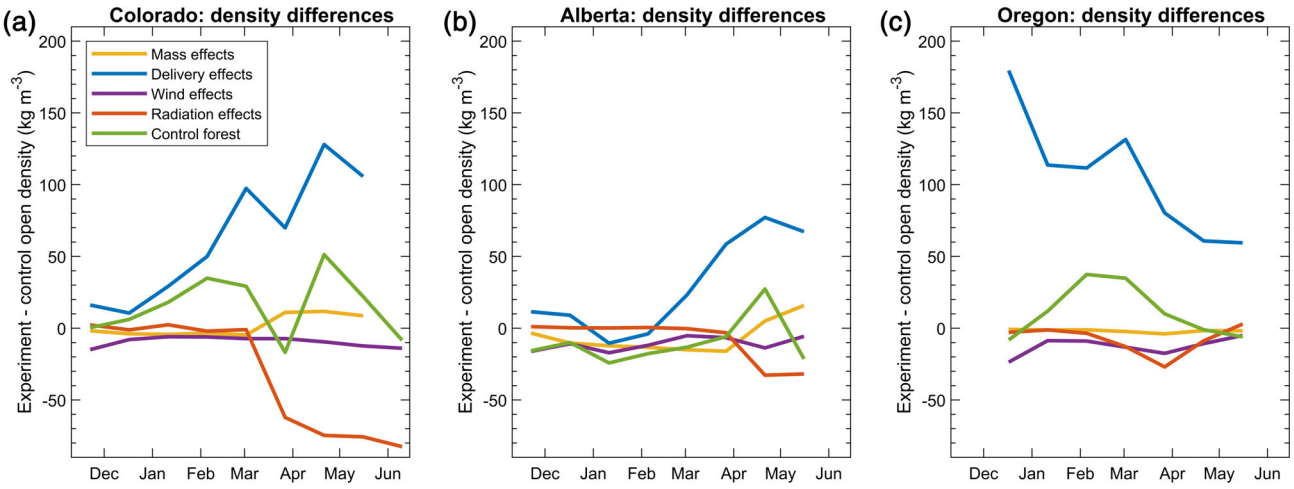

FIGURE 9 Density differences between model experiments and control open at the three study sites during a typical water year (Colorado, WY 2015; Alberta, WY 2014; Oregon, WY 2013). Density differences between control forest and control open are also shown. Results are smoothed by calculating median values over a 25-day period. Density values are only shown when snowpack is at least 15 cm in depth

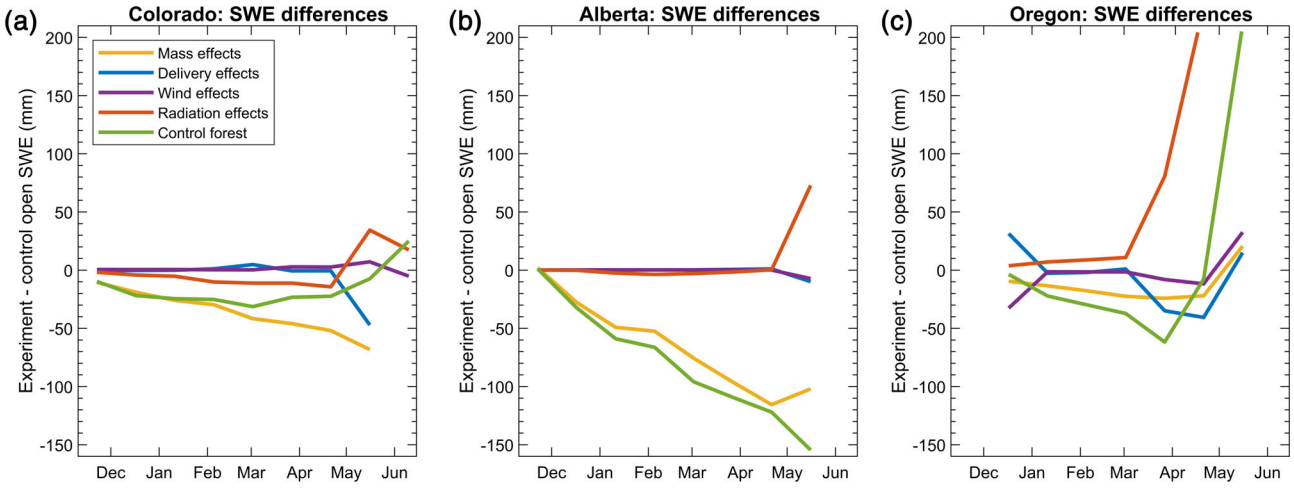

FIGURE 10 SWE differences between model experiments and control open at the three study sites during a typical water year (Colorado, WY 2015; Alberta, WY 2014; Oregon, WY 2013). SWE differences between control forest and control open are also shown. Results are smoothed by calculating median values over a 25-day period. Density values are only shown when snowpack is at least 15 cm in depth

4.4 | Delivery effects experiment

4.4.1 | Density

Delivery effects yielded increased snow density at all sites, years, and seasons (Figures 7, 9). The simulated changes in density from delivery effects were the largest of the four experiments and increased experiment density by up to 60% relative to control open (Figure 7). Delivery effects were most pronounced at Oregon, small to intermediate at Alberta, and small at Colorado, consistent with the prescribed changes in density and method of delivered water (Figure 2a). At Colorado and Alberta, delivery effects were greatest late in the snow year (Figure 9), when melt of intercepted snow was highest. Melt of intercepted snow occurred all season at Oregon, thus the changes in density were high throughout the year but most pronounced earlier in the year when control open density was lowest. In the sensitivity experiments, we varied drip amount by ±20%. This modified the density of unloaded material, yielding DM change of up to 16%. However, the relative magnitude of delivery effects compared to the other experiments and control forest remained consistent even when model sensitivity was considered.

4.4.2 | Snow water equivalent

Although the amount of snow mass was not altered in the delivery effects experiment, changes in SWE occurred from greater liquid content and propensity to melt. SWE differences between the delivery effects experiment and control open at Colorado and Alberta were typically near zero (Figure 8). At Oregon, delivery effects reduced SWE between 0% and 28%. At this site, the increased density of snow

delivered to the snowpack yielded greater liquid water content and drainage during mid-season melt events (e.g., decreased March–April SWE for delivery effects experiment versus control open in Figure 10c), resulting in years with larger, negative SMs. The delivery effects experiment during one exceptionally low snow year at Oregon melted too rapidly to have enough data to calculate a reasonable SM or DM. Cool and wet years at Oregon and an unusually dry year at Colorado tended to be the most responsive to sensitivity experiments changing liquid drip ratio.

4.5 | Wind effects experiment

4.5.1 | Density

The wind effects experiment (lower wind under the forest canopy, and thus lower new snow density) reduced snow density at all sites and during all years (Figures 7, 9), resulting in density 2%–7% lower than control open. The wind effects experiments were only slightly sensitive to varying the selected minimum new snow density parameter from 50 to 100 kg m^{-3}, and maintained the relationship seen using the default parameter when compared to other experiments.

4.5.2 | Snow water equivalent

While the wind effects experiment did not directly alter the amount of snow mass, minor changes in SWE were apparent from reduced snow density and consequent faster melt rate (Figure 8). This experiment consistently resulted in low magnitude SMs (<10% decrease for all but 1 year). SMs were not sensitive to varying the minimum new snow density parameter.

4.6 | Radiation effects experiment

4.6.1 | Density

Introduction of a forest canopy radiation regime both increased density by accelerating grain growth and compaction (e.g., greater net radiation and warmer surface temperature until mid-May for all sites in Figure 3) and decreased density by limiting melt-refreeze cycles and delaying melt (this was evident during the ablation season at Colorado, see Figure 9a). Combined, these processes were frequently offsetting, as indicated by near-zero DMs (Figure 7). At Colorado and Alberta, the radiation effects experiment had DMs between 0% and 4% for all but 1 year. At Oregon, the radiation effects experiment had a larger impact on density differences with DM values as high as 22%. The radiation effects experiment was the most responsive to our sensitivity experiments. Changing the amount of incoming radiation by ±5% led DM values to vary by up to 15%. However, considering sensitivity did not generally change the overall significance of radiation effects compared to other processes.

4.6.2 | Snow water equivalent

Radiation effects decreased SWE by 0%–5% relative to control open at Colorado, and increased SWE by 2%–43% relative to control open at Alberta and Oregon (Figure 8). This varying response was likely correlated to site radiation regimes, including greater net radiation differences between control forest and open at Alberta and Oregon (Figure 3g–i), and their influence on the timing of melt. SM response to experiment sensitivity was high. Perturbing the amount of incoming radiation had the potential to change SMs by up to 20% at Colorado and Alberta and up to 65% at Oregon. Results varied widely within the sensitivity range for all sites: radiation effects SMs could be reversed in sign or near negligible. This high level of sensitivity was expected, as radiation fluxes were highly influential on the timing of SWE loss.

5 | DISCUSSION

Our modelling experiments examined how forest canopies impact snowpack density and SWE. Previous studies have speculated about the competing effects of these forest processes (e.g., Lundberg & Koivusalo, 2003; Rasmus, 2013), but to our knowledge this is the first study to isolate the impact of these processes on snow density.

The mass effects experiment showed that canopy interception loss reduced snow mass on the ground, and thus reduced overburden compaction and bulk density in the forest relative to the open. This effect caused bulk density decreases of 10% for typical interception losses. The reason for this low magnitude decrease is that overburden compaction rates decrease with increasing snow density (Figure 1a-b), and therefore mass effects are most important for lower-density snow (< ~250 kg m^{-3}). This is why mass effects were largest at Alberta, where snow density tended to be lower than the other two sites (Figure 4). The low magnitude of our mass effects DMs is consistent with Sturm and Holmgren (1998), who found that density in a viscous-compaction model was less sensitive to mass effects than to other factors.

The delivery effects experiment consistently yielded the largest density changes. Even considering sensitivity, DMs were 5–15 times larger for delivery effects than other experiments. The greatest changes in density occurred at the warmest times in the snow season, when intercepted snow melted in the canopy and drained to the snowpack as liquid water. This unloading created high density layers that persisted on the timescale of months (Figure 5b). At Colorado and Alberta, this happened in late winter and spring. The warmer climate at Oregon kept liquid drainage as the dominant pathway for canopy water unloading throughout the year. Limited literature is available on the magnitude of melt drip, but our high incoming snow density at Oregon (Figure 2a) is consistent with results from Storck et al. (2002) who found that 72% of unloaded, intercepted snow was removed as meltwater drip in their maritime site. Delivery effects were most important in years with many smaller storms rather than several big storms (not shown). When a storm's total precipitation far

exceeded interception capacity, most of the precipitation was throughfall and could not be affected by delivery effects, thereby reducing meltwater drip (Floyd & Weiler, 2008).

The wind effects experiment showed that faster wind speeds increased new snow density in the open (Figure 1c), resulting in relatively lower forest snow density. This effect was seen most during large storm events with high wind speeds and a shallow preexisting snowpack. Our results align with expectations from other studies (Pahaut, 1976; Pomeroy & Gray, 1995) and may have yielded larger DMs had wind drifting also been considered. Wind effects usually yielded higher magnitude DMs than radiation effects and similar to larger magnitude DMs than mass effects.

The radiation effects experiment illustrated competing outcomes of the forest radiation regime on snow densification. Less extreme diurnal fluctuations in net radiation in the forest reduced densification from melt-freeze cycles, while overall greater forest net radiation during most of the snow season increased densification by increasing the rate of overburden compaction (Balk & Elder, 2000; Dickerson-Lange et al., 2017; Lundquist et al., 2013). These competing effects tended to offset, resulting in small DMs, with the exception of 2 years at Oregon. Because the radiation effects experiment changed the timing and duration of melt, the simulated differences in density also reflected changes in the temporal evolution of SWE and melt state.

For each effect, we also examined the sensitivity of experiment results. For forest-to-open density differences, interannual variability is similar to experiment sensitivity. With the exception of radiation effects, for forest-to-open SWE differences, experiment sensitivity is less than interannual variability. Some radiation effects SMs varied in the sensitivity experiments by more than 30% at Oregon, but generally both DM and SM sensitivity was less than 10% for most experiments at all sites.

In summary, the model experiments suggest that delivery effects increase forest snowpack density relative to open areas; mass and wind effects decrease forest snowpack density; and radiation effects either increase or have relatively minor influence on forest-open differences in density. In contrast, mass effects have the greatest impact on SWE, lowering it throughout the water year. Depending on the year and site, radiation effects may also have a large magnitude impact on SWE. Radiation effects explain changes in seasonal SWE and may shift the onset of melt by over a month (Figure 10c).

The four experiments were designed to isolate individual effects of canopies on the underlying snowpack. All four effects act simultaneously in the control forest simulation, and thus interactions between them exist. SUMMA predicted that control forest had higher bulk density than control open at Colorado and Oregon, and similar to slightly lower bulk density as control open for most years at Alberta (Figure 7; low magnitude of density differences at Alberta similar to those found by Lv & Pomeroy, 2020). Differences between control forest and control open must largely be driven by delivery effects, tempered by mass and wind effects. However, the simulated change in density resulting from delivery effects (a DM of ~10%–50%) minus mass effects (~1%–12%) and wind effects (~2%–6%) was larger than differences between control forest and open (~2%–24%). Thus, delivery effects, as simulated in the experiment, are moderated by the interactions between all processes in control forest.

6 | CONCLUSION

Experiments showed that forest delivery effects – the unloading of snow and liquid melt from the canopy – had the largest impact on bulk snow density (Figure 7). Delivery effects consistently increased density, often by 20%–60% compared to the open. This delivery effect was greatest during the warmer parts of the snow season and at the warmest site. Radiation effects had a negligible to positive impact on forest snowpack density, increasing it by 0%–23%. Mass effects and wind effects decreased forest snowpack density by 1%–12% and 2%–6%, respectively.

The experiments also resulted in changes to SWE (Figure 8). Radiation and mass effects were the greatest drivers of SWE differences between open and forested sites. Mass effects reduced SWE by 4%–36% and were largely governed by the amount of incoming precipitation intercepted and lost by sublimation or evaporation. By changing the timing of melt, radiation effects had a more variable impact, decreasing SWE by up to 5% and increasing SWE by up to 43%. Delivery and wind effects were minor, generally reducing SWE by less than 10%.

Our results illustrate the antithetical effects of forest processes on snowpack density and SWE, with particular emphasis on the importance of delivery effects. We conclude that accurate process representation, informed by more holistic observations of unloaded snow properties in forests, is key to modelling snowpack density. In turn, improved representation of densification processes across landscapes will advance the accuracy of SWE mapping from measured snow depth and modelled snow density.

ACKNOWLEDGEMENTS

This work was supported by the National Science Foundation Hydrologic Sciences Program under Grant No. 1761441. Any opinions, findings, and conclusions or recommendations expressed in this material are those of the author(s) and do not necessarily reflect the views of the National Science Foundation. Logistical support for data collection on Snodgrass Mountain was facilitated by the Department of Energy WFSFA, the Rocky Mountain Biological Laboratory, and the USDA Forest Service. We acknowledge the 2019 field observers at Snodgrass: E. Smyth, A. Michell, V. Foley, J. Kaschinske, E. Cruise, and L. Coe, and field researchers at the Oregon and Alberta sites.

DATA AVAILABILITY STATEMENT

The data that support the findings of this study are available from the corresponding author upon reasonable request.

ORCID

Hannah M. Bonner https://orcid.org/0000-0002-8257-2007
Eric E. Small https://orcid.org/0000-0002-5010-4954

REFERENCES

Anderson, E. A. (1976). A point energy and mass balance model of a snow cover. *NOAA Technical Report NWS; 19*.

Andreadis, K. M., Storck, P., & Lettenmaier, D. P. (2009). Modeling snow accumulation and ablation processes in forested environments. *Water Resources Research*, *45*(5), W05429. https://doi.org/10.1029/2008WR007042

Bader, H. (1960). Theory of densification of dry snow on high polar glaciers. *CRREL Research Report*, *69*, 1–8.

Balk, B., & Elder, K. (2000). Combining binary decision tree and geostatistical methods to estimate snow distribution in a mountain watershed. *Water Resources Research*, *36*(1), 13–26.

Bavay, M., & Egger, T. (2014). MeteoIO 2.4.2: A preprocessing library for meteorological data. *Geoscientific Model Development*, *7*, 3135–3151.

Bormann, K. J., Westra, S., Evans, J. P., & McCabe, M. F. (2013). Spatial and temporal variability in seasonal snow density. *Journal of Hydrology*, *484*, 63–73.

Bründl, M., Schneebeli, M., & Flühler, H. (1999). Routing of canopy drip in the snowpack below a spruce crown. *Hydrological Processes*, *13*(1), 49–58.

Chen, S., & Baker, I. (2010). Evolution of individual snowflakes during metamorphism. *Journal of Geophysical Research Atmospheres*, *115*(21), D21114. https://doi.org/10.1029/2010JD014132

Clark, M. P., Nijssen, B., Lundquist, J. D., Kavetski, D., Rupp, D. E., Woods, R. A., … Marks, D. G. (2015b). A unified approach for process-based hydrological modeling: 2. Model implementation and case studies. *Water Resources Research*, *51*(4), 2515–2542.

Clark, M. P., Nijssen, B., Lundquist, J. D., Kavetski, D., Rupp, D. E., Woods, R. A., … Rasmussen, R. M. (2015a). A unified approach for process-based hydrological modeling: 1. *Modeling concept*. *Water Resources Research*, *51*(4), 2498–2514.

Colbeck, S. C. (1982). An overview of seasonal snow metamorphism. *Reviews of Geophysics*, *20*(1), 45–61.

Crawford, J. L., Mcnulty, S. P., Sowell, J. B., & Morgan, M. D. (1998). Changes in aspen communities over 30 years in Gunnison County. *Colorado*. *The American Midland Naturalist*, *140*(2), 197–205.

Deems, J. S., Painter, T. H., & Finnegan, D. C. (2013). Lidar measurement of snow depth: A review. *Journal of Glaciology*, *59*(215), 467–479.

Dickerson-Lange, S. E., Gersonde, R. F., Hubbart, J. A., Link, T. E., Nolin, A. W., Perry, G. H., … Lundquist, J. D. (2017). Snow disappearance timing is dominated by forest effects on snow accumulation in warm winter climates of the Pacific northwest. *United States*. *Hydrological Processes*, *31*(10), 1846–1862.

Dickinson, R. E. (1983). Land surface processes and climate-surface albedos and energy balance. *Advances in Geophysics*, *25*, 305–353.

Elder, K., Brucker, L., Hiemstra, C., & Marshall, H. (2018). *SnowEx17 community snow pit measurements*, *version 1*. NASA National Snow and Ice Data Center Distributed Active Archive Center.

Essery, R. (2015). A factorial snowpack model (FSM 1.0). *Geoscientific Model Development*, *8*, 6583–6609.

Essery, R., Pomeroy, J., Ellis, C., & Link, T. (2008). Modelling longwave radiation to snow beneath forest canopies using hemispherical photography or linear regression. *Hydrological Processes*, *22*(15), 2788–2800.

Fang, X., Pomeroy, J. W., DeBeer, C. M., Harder, P., & Siemens, E. (2019). Hydrometeorological data from Marmot Creek Research Basin, Canadian Rockies. *Earth System Science Data*, *11*, 455–471.

Floyd, W., & Weiler, M. (2008). Measuring snow accumulation and ablation dynamics during rain-on-snow events: Innovative measurement techniques. *Hydrological Processes*, *22*(24), 4805–4812.

Gray, J. T., & Morland, L. W. (1995). The compaction of polar snow packs. *Cold Region Science Technology*, *23*, 109–119.

Harding, R., & Pomeroy, J. W. (1996). The energy balance of the winter boreal landscape. *Journal of Climate*, *9*, 2778–2787.

Hardy, J. P., Melloh, R., Koenig, G., Marks, D., Winstral, A., Pomeroy, J. W., & Link, D. (2004). Solar radiation transmission through conifer canopies. *Agricultural and Forest Meterorology*, *126*(3–4), 257–270.

Harpold, A. A., Guo, Q., Molotch, N., Brooks, P. D., Bales, R., Fernandez-Diaz, J. C., … Lucas, R. (2014). LiDAR-derived snowpack data sets from mixed conifer forests across the Western United States. *Water Resources Research*, *50*, 2749–2755.

Hedstrom, N. R., & Pomeroy, J. W. (1998). Measurements and modelling of snow interception in the boreal forest. *Hydrological Processes*, *12*, 1611–1625.

Hopkinson, C., Demuth, M. N., Sitar, M., & Chasmer, L. E. (2001). Applications of airborne LiDAR mapping in glacierised mountainous terrain. *Proceedings of the International Geoscience and Remote Sensing Symposium*, *2*, 949–951. https://doi.org/10.1109/IGARSS.2001.976690

Jordan, R. E (1991). A one-dimensional temperature model for snow cover. Technical documentation for SNTHERM, Special Report, 89.

Judson, A., & Doesken, N. (2000). Density of freshly fallen snow in the central Rocky Mountains. *Bulletin of the American Meteorological Society*, *81*(7), 1577–1588.

Kozlov, M. V. (2001). Snowpack changes around a nickel-copper smelter at Monchegorsk, northwestern Russia. *Canadian Journal of Forest Research*, *31*, 1684–1690.

Lafaysse, M., Cluzet, B., Dumont, M., Lejeune, Y., Vionnet, V., & Morin, S. (2017). A multiphysical ensemble system of numerical snow modelling. *The Cryosphere*, *11*(3), 1173–1198.

Lawler, R. R., & Link, T. E. (2011). Quantification of incoming all-wave radiation in discontinuous forest canopies with application to snowmelt prediction. *Hydrological Processes*, *25*(21), 3322–3331.

Lawrence, D. M., Oleson, K. W., Falnner, M. G., Thornton, P. E., Swenson, S. C., Lawrence, P. J., … Slater, A. G. (2011). Parameterization improvements and functional and structural advances in version 4 of the community land model. *Journal of Advances in Modeling Earth Systems*, *3*(1), M03001. https://doi.org/10.1029/2011MS00045

Lehning, M., Bartelt, P., Brown, B., Fierz, C., & Satyawali, P. (2002). A physical SNOWPACK model for the Swiss avalanche warning part II. Snow microstructure. *Cold Regions Science and Technology*, *35*, 147–167.

Liston, G. E., & Sturm, M. (1998). A snow-transport model for complex terrain. *Journal of Glaciology*, *44*, 498–516.

Lundberg, A., Calder, I., & Harding, R. (1997). Evaporation of intercepted snow: Measurement and modeling. *Journal of Hydrology*, *206*, 151–163.

Lundberg, A., Gustafsson, D., Stumpp, C., Kløve, B., & Feiccabrino, J. (2016). Spatiotemporal variations in snow and soil frost—A review of measurement techniques. *Hydrology*, *3*(3), 28. https://doi.org/10.3390/hydrology3030028

Lundberg, A., & Koivusalo, H. (2003). Estimating winter evaporation in boreal forests with operational snow course data. *Hydrological Processes*, *17*(8), 1479–1493.

Lundberg, A., Richardson-Naslund, C., & Andersson, C. (2006). Snow density variations: Consequences for ground-penetrating radar. *Hydrological Processes*, *20*, 1483–1495.

Lundquist, J. D., Dickerson-Lange, S. E., Lutz, J. A., & Cristea, N. C. (2013). Lower forest density enhances snow retention in regions with warmer winters: A global framework developed from plot-scale observations and modeling. *Water Resource Research*, *49*, 6356–6370.

Lv, Z., & Pomeroy, J. W. (2020). Assimilating snow observations to snow interception process simulations. *Hydrological Processes*, *34*(10), 2229–2246.

Mahat, V., & Tarboton, D. G. (2012). Canopy radiation transmission for an energy balance snowmelt model. *Water Resources Research*, *48*(1).

Male, D. H., Gray, D. M. (1981). Handbook of snow: principles, processes, management and use

Marchand, W. D., & Killingtveit, A. (2004). Statistical properties of spatial snowcover in mountainous catchments in Norway. *Nordic Hydrology*, *35*(2), 101–117.

Marks, D., & Winstral, A. (2001). Comparison of snow deposition, the snow cover energy balance, and snowmelt at two sites in a semiarid mountain basin. *Journal of Hydrometeorology*, *2*, 213–227.

McCreight, J. C., & Small, E. E. (2014). Modeling bulk density and snow water equivalent using daily snow depth observations. *The Cryosphere*, *8*, 521–536.

Mizukami, N., & Perica, S. (2008). Spatiotemporal characteristics of snowpack density in the mountainous regions of the Western United States. *Journal of Hydrometeorology*, *9*, 1416–1426.

Oswalt, S. N., Smith, W. B. (2014). U.S. forest resource facts and historical trends. USDA Forest Service, FS-1035.

Pahaut, E. (1976). *La métamorphose des cristaux de neige (Snow crystal metamorphosis)*. Monographies de la Météorologie Nationale.

Painter, T., Berisford, D., Boardman, J., Bormann, K., Deems, J., Gehrke, F., … Winstral, A. (2016). The airborne snow observatory: Fusion of scanning lidar, imaging spectrometer, and physically-based modeling for mapping snow water equivalent and snow albedo. *Remote Sensing of the Environment*, *184*, 139–152.

Peterson, N. R., & Brown, A. J. (1975). Accuracy of snow measurements. *Proceedings of the 43rd Western Snow Conference*, 1–5.

Pomeroy, J., Demuth, M., Helgason, W., & Westbrook, C. (2013). *Marmot Creek, Peyto glacier and the Canadian Rockies hydrological observatory*. Presentation at CCRN's Targeted Process Studies Workshop. http://ccrnetwork.ca/science/WECC/western-cordillera/marmot-creek.php

Pomeroy, J. W., & Gray, D. M. (1995). Snowcover accumulation, relocation and management. *National Hydrology Research Institute Science*, 135.

Rasmus, S. (2013). Spatial and temporal variability of snow bulk density and seasonal snow densification behavior in Finland. *Geophysica*, *49*(1–2), 53–74.

Raymond, C., & Tusima, K. (1979). Grain coarsening of water saturated snow. *Journal of Glaciology*, *22*(86), 83–105.

Roth, T. R., & Nolin, A. W. (2017). Forest impacts on snow accumulation and ablation across an elevation gradient in a temperate montane environment. *Hydrology and Earth System Sciences*, *21*, 5427–5442.

Roth, T. R., & Nolin, A. W. (2019). Characterizing maritime snow canopy interception in forested mountains. *Water Resources Research*, *55*, 4564–4581.

Rutter, N., Essery, R., Pomeroy, J., Altimir, N., Andreadis, K., Baker, I., … Yamazaki, T. (2009). Evaluation of forest snow processes models (SnowMIP2). *Journal of Geophysical Research*, *114*, 1–18.

Schöber, J., Achleitner, S., Bellinger, J., Kirnbauer, R., & Schöberl, F. (2016). Analysis and modelling of snow bulk density in the tyrolean alps. *Hydrology Research*, *42*(2), 419–441.

Sellers, P. (1985). Canopy reflectance, photosynthesis and transpiration. *International Journal of Remote Sensing*, *6*(8), 1335–1372.

Sicart, J. E., Essery, R. L., Pomeroy, J. W., Hardy, J., Link, T., & Marks, D. (2004). A sensitivity study of daytime net radiation during snowmelt to forest canopy and atmospheric conditions. *Journal of Hydrology*, *5*(5), 774–784.

Sommer, C. G. (2018). Wind-packing of snow: How do wind crusts form? PhD Thesis, no. 8628, EPFL, Switzerland

Sommer, C. G., Wever, N., Fierz, C., & Lehning, M. (2018). Investigation of a wind-packing event in Queen Maud Land, Antarctica. *The Cryosphere*, *12*(9), 2923–2939. https://doi.org/10.5194/tc-12-2923-2018

Spittlehouse, D. I., & Winkler, R. D. (1996). Forest canopy effects on sample size requirements in snow accumulation and melt comparisons. *Proceedings of the 64th Western Snow conference*, 39–46.

St. Clair, J., & Holbrook, W. S. (2017). Measuring snow water equivalent from common-offset GPR records through migration velocity analysis. *The Cryosphere*, *11*, 2997–3009.

Storck, P., Lettenmaier, D. P., & Bolton, S. M. (2002). Measurement of snow interception and canopy effects on snow accumulation and melt in a mountainous maritime climate, Oregon, United States. *Water Resources Research*, *38*, 1–16.

Stoy, P. C., Peitzsch, E. H., Wood, D. J. A., Rottinghaus, D., Wohlfahrtd, G., Goulden, M., & Ward, H. (2018). On the exchange of sensible and latent heat between the atmosphere and melting snow. *Agricultural and Forest Meteorology*, *252*, 167–174.

Sturm, M., & Holmgren, J. (1998). Differences in compaction behavior of three climate classes of snow. *Annals of Glaciology*, *26*, 125–130.

Sturm, M., Holmgren, J., & Liston, G. E. (1995). A seasonal snowcover classification system for local to global applications. *Journal of Climatology*, *8*(5), 1261–1283.

Sturm, M., Liston, G. E., Benson, C. S., & Holmgren, J. (2001). Characteristics and growth of a snowdrift in arctic Alaska, U.S.A. *Arctic, Antarctic, and Alpine Research*, *33*(3), 319–329.

Teich, M., Giunta, A. D., Hagenmuller, P., Bebi, P., Schneebeli, M., & Jenkins, M. J. (2019). Effects of bark beetle attacks on forest snowpack and avalanche formation – Implications for protection forest management. *Forest Ecology and Management*, *438*, 186–203.

Terzago, S., Andreoli, V., Arduini, G., Balsamo, G., Campo, L., … Provenzale, A. (2020). Sensitivity of snow models to the accuracy of meteorological forcings in mountain environments. *Hydrology and Earth System Sciences*, *24*(8), 4061–4090.

Timoney, K., Kershaw, G. P., & Olesen, D. (1992). Late winter snow-landscape relationships in the subarctic near Hoarfrost River, Great Slave Lake, Northwest Territories, Canada. *Water Resource Research*, *28*(7), 1991–1998.

Trujillo, E., & Molotch, N. P. (2014). Snowpack regimes of the Western United States. *Water Resources Rsearch*, *50*, 5611–5623.

Varhola, A., Coops, N. C., Weiler, M., & Moor, R. D. (2010). Forest canopy effects on snow accumulation and ablation: An integrative review of empirical results. *Journal of Hydrology*, *392*, 219–233.

Vionnet, V., Brun, E., Morin, S., Boone, A., Faroux, S., Le Moigne, P., … Willemet, J. M. (2012). The detailed snowpack scheme crocus and its implementation in SURFEX v7.2. *Geoscience Model Development*, *5*, 773–791.

Watson, F., Anderson, T., Newman, W., Alexander, S., & Garrott, R. (2006). Optimal sampling schemes for estimating mean snow water equivalents in stratified heterogenous landscapes. *Journal of Hydrology*, *328*, 432–452.

Wayand, N. E., Clark, M. P., & Lundquist, J. D. (2017). Diagnosing snow accumulation errors in a rain-snow transitional environment with snow board observations. *Hydrological Processes*, *31*(2), 349–363.

Webb, R. W., Raleigh, M. S., McGrath, D., Molotch, N. P., Elder, K., Hiemstra, C., Brucker, L., & Marshall, H. P. (2020). Within-stand boundary effects of snow water equivalent distribution in forested areas. *Water Resources Research.*, *56*, e2019WR024905. https://doi.org/10.1029/2019WR024905

Winstral, A., & Marks, D. (2014). Long-term snow distribution observations in a mountain catchment: Assessing variability, time stability, and the representativeness of an index site. *Water Resources Research*, *50*, 1–13.

Xia, Y., Mitchell, K., Ek, M., Sheffield, J., Cosgrove, B., Wood, E., … Mocko, D. (2012). Continental-scale water and energy flux analysis and validation for the north American land data assimilation system project phase 2 (NLDAS-2): 1. Intercomparison and application of model products. *Journal of Geophysical Research*, *117*(D3), 1–27.

SUPPORTING INFORMATION

Additional supporting information may be found in the online version of the article at the publisher's website.

How to cite this article: Bonner, H. M., Raleigh, M. S., & Small, E. E. (2022). Isolating forest process effects on modelled snowpack density and snow water equivalent. *Hydrological Processes*, *36*(1), e14475. https://doi.org/10.1002/hyp.14475